



# Hydrothermal mass production of $\text{MgBO}_2(\text{OH})$ nanowhiskers and subsequent thermal conversion to $\text{Mg}_2\text{B}_2\text{O}_5$ nanorods for biaxially oriented polypropylene resins reinforcement

Wancheng Zhu<sup>a,b,\*</sup>, Guangdong Li<sup>a</sup>, Qiang Zhang<sup>a</sup>, Lan Xiang<sup>a,\*</sup>, Shenlin Zhu<sup>a</sup>

<sup>a</sup> Department of Chemical Engineering, Tsinghua University, Beijing 100084, China

<sup>b</sup> Department of Chemical Engineering, Qufu Normal University, Shandong 273165, China

## article info

### Article history:

Received 27 February 2010

Received in revised form 3 May 2010

Accepted 14 May 2010

Available online 21 May 2010

### Keywords:

Magnesium borates

Hydrothermal

Calcination

Nanomaterials

Mass production

## abstract

Mass production of one-dimensional (1D) nanomaterials has emerged as one of the most significant challenges in powder technology. In this contribution,  $\text{MgBO}_2(\text{OH})$  nanowhiskers were hydrothermally produced at a kilogram scale in a 150 L stainless steel autoclave at 200 °C for 12.0 h by using  $\text{MgCl}_2 \cdot 6\text{H}_2\text{O}$ ,  $\text{H}_3\text{BO}_3$  and  $\text{NaOH}$  as the raw materials. The subsequent thermal conversion of the  $\text{MgBO}_2(\text{OH})$  nanowhiskers at 700 °C for 6 h led to 3.75 kg of high crystallinity monoclinic  $\text{Mg}_2\text{B}_2\text{O}_5$  nanorods, with a length of 0.47–1.3  $\mu\text{m}$ , a diameter of 55–160 nm, and an aspect ratio of 3–15. After the nanorods have been surface modified with the silane coupling agent KH-550, the reinforcing and toughening effects of the  $\text{Mg}_2\text{B}_2\text{O}_5$  nanorods on the biaxially oriented polypropylene resins (BOPP-D1) were evaluated. The filling of the  $\text{Mg}_2\text{B}_2\text{O}_5$  nanorods into the resins resulted in the increase in the tensile strength, the impact strength, and the melt flow index of the BOPP-D1 composites. The appropriate ratio of coupling agent to fillers ( $\text{Mg}_2\text{B}_2\text{O}_5$  nanorods) and the ratio of fillers to resins were determined within the range of 0.6–1.2 wt.% and 8–15 wt.%, respectively. The optimal ratio of fillers to resins was ca. 10 wt.%. The present mass production of  $\text{MgBO}_2(\text{OH})$  nanowhiskers and  $\text{Mg}_2\text{B}_2\text{O}_5$  nanorods is believed to be helpful for enlarging and propelling the applications of the 1D magnesium borate nanostructures in the near future.

© 2010 Elsevier B.V. All rights reserved.

## 1. Introduction

Originating from the small size, cylindrical structure, and high aspect ratio, one-dimensional (1D) nanostructures such as nanotubes, nanowires, nanorods, and nanobelts have been one of the focuses of intensive research. For example, carbon nanotubes (CNTs),  $\text{CaCO}_3$ ,  $\text{ZnO}$ ,  $\text{TiO}_2$  and  $\text{Mg}(\text{OH})_2$  have been successfully applied to composite materials in plastic, rubber and metal matrixes [1,2], in catalysis [3], in energy conversion and storage [4,5], and in many other areas. 1D nanostructured magnesium borates, including  $\text{MgB}_4\text{O}_7$  nanowires [6],  $\text{Mg}_3\text{B}_2\text{O}_6$  nanotubes [7] and nanobelts [8],  $\text{Mg}_2\text{B}_2\text{O}_5$  nanowires [9,10], nanorods [11], and whiskers [12], etc., have been paid much attention in recent years for their potential usages as reinforcements in the electronic ceramics [6], wide band gap semiconductors [9], antiwear additives [10], and plastics or aluminum/magnesium matrix alloys [12–14]. The demand for such raw materials is rising explosively. Mass production of nanomaterials with a full size and morphology control has emerged as one of the most significant challenges in modern chemical engineering.

Up to now, powder technology plays a key role in mass production of various 1D nanomaterials [15–18]. For example, various kinds of CNTs, such as single walled [15], few walled [19], multi-walled [15,20], and aligned CNTs [21,22], have been successfully mass produced in fluidized bed; nanoparticles such as  $\text{CaCO}_3$  were mass produced within the rotating packed bed by the high gravity reactive precipitation technology [17,23,24].  $\text{ZnO}$  nanotetrapods [25] and nanotripods [26] via the flowing gas phase reaction method or chemical vapor deposition, etc., have also been recently realized or effectively endeavored. Among various synthetic strategies for 1D micro-/nanostructured materials, hydrothermal technology has been recognized as a thriving approach for 1D nanostructures in the last decade, owing to its advantages over other conventional processes such as energy saving, better control of nucleation and shape, and lower temperature of operation, etc. [27–30]. In our previous work, uniform pore-free high crystallinity  $\text{Mg}_2\text{B}_2\text{O}_5$  nanowhiskers with twin crystal structures have been successfully obtained via a flux-assisted thermal conversion route at a relatively low temperature as 650–700 °C [31], on the basis of the hydrothermal synthesis of the uniform  $\text{MgBO}_2(\text{OH})$  nanowhiskers [32]. However, the previous work could only get ca. 1 g of  $\text{MgBO}_2(\text{OH})$  nanowhiskers in each hydrothermal synthesis. Absolutely, a larger quantity of the  $\text{Mg}_2\text{B}_2\text{O}_5$  nanowhisker samples was inevitably needed for further application exploration,

\* Corresponding authors. Department of Chemical Engineering, Qufu Normal University, Shandong 273165, China. Fax: + 86 10 6277 2051.

E-mail addresses: [zhuwancheng@tsinghua.org.cn](mailto:zhuwancheng@tsinghua.org.cn) (W. Zhu), [xianglan@mail.tsinghua.edu.cn](mailto:xianglan@mail.tsinghua.edu.cn) (L. Xiang).

whereas it was few reported for mass production of the nanomaterials by the hydrothermal route to date.

In this contribution, we report the mass production of  $\text{MgBO}_2(\text{OH})$  nanowhiskers and  $\text{Mg}_2\text{B}_2\text{O}_5$  nanorods by a hydrothermal-calcination route, in which the  $\text{MgBO}_2(\text{OH})$  nanowhiskers were hydrothermally synthesized by using a 150 L stainless steel autoclave and the  $\text{Mg}_2\text{B}_2\text{O}_5$  nanorods were obtained by the subsequent thermal conversion. The reinforcing and toughening effects of the  $\text{Mg}_2\text{B}_2\text{O}_5$  nanorods on the biaxially oriented polypropylene (BOPP-D1) resins were also investigated.

## 2. Experimental

### 2.1. Mass production of $\text{MgBO}_2(\text{OH})$ nanowhiskers and $\text{Mg}_2\text{B}_2\text{O}_5$ nanorods

A stainless steel autoclave with the capacity of 150 L was used for the hydrothermal mass production. All of the reagents were purchased in the analytical grade without further purification. As shown in Fig. 1, 32.56 L of  $\text{MgCl}_2$  ( $2.0 \text{ mol L}^{-1}$ ) was mixed with 32.56 L of  $\text{H}_3\text{BO}_3$  ( $3.0 \text{ mol L}^{-1}$ ) firstly, the mixture was then supplied with deionized (DI) water and subsequently dropwise added 32.56 L of  $\text{NaOH}$  ( $4.0 \text{ mol L}^{-1}$ ) for room temperature coprecipitation by using a plastic pail with specially decorated four ball valves at the bottom under vigorous mechanical stirring (ca. 180 rpm), leading to 100 L of hydrothermal precursor slurry. The precursor slurry was then transferred into a 150 L stainless steel autoclave equipped with a bursting disc and a precise temperature control system, under mechanical stirring (ca. 150 rpm). The autoclave was sealed and heated to  $200^\circ\text{C}$  ( $40^\circ\text{C}$  lower than that used for the previous hydrothermal gram-scale synthesis [32], so as to reduce the possible corrosion of chlorine ions) and kept at the isothermal condition for 12.0 h. After the hydrothermal treatment, the autoclave was cooled down to room temperature naturally. The slurry containing the hydrothermal product was collected from the outlet located at the bottom of the autoclave, and then transferred into a tripod centrifuge in three batches for further washing and purification of the hydrothermal product. The wet powder was finally collected and moved to a box-type oven for drying at  $105\text{--}110^\circ\text{C}$  for 12.0 h, resulting kilogram-scale hydrothermally synthesized  $\text{MgBO}_2(\text{OH})$  nanowhiskers. The  $\text{MgBO}_2(\text{OH})$  nanowhiskers were ultimately transferred into a muffle furnace and calcined in batches for thermal conversion to form  $\text{Mg}_2\text{B}_2\text{O}_5$  nanorods at  $700^\circ\text{C}$  for 6.0 h.

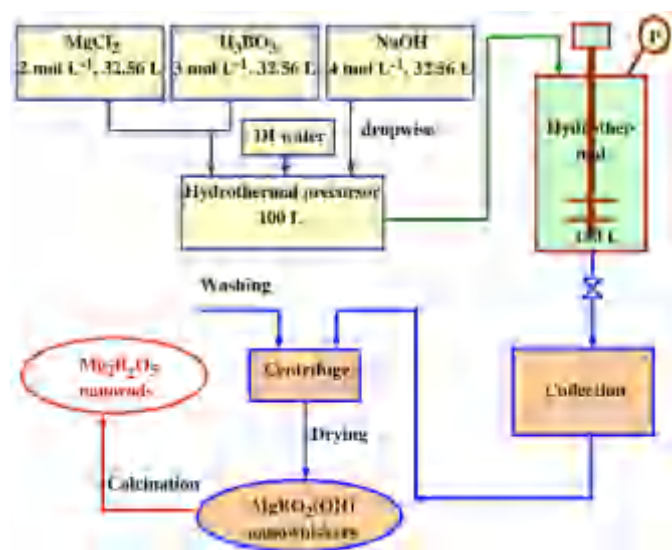


Fig. 1. Sketch map of the kilogram-scale synthetic route to  $\text{MgBO}_2(\text{OH})$  nanowhiskers and  $\text{Mg}_2\text{B}_2\text{O}_5$  nanorods.

For comparison, a gram-scale synthetic route to  $\text{MgBO}_2(\text{OH})$  nanowhiskers with the same concentration of the reactants as that utilized in the mass production was performed as follows: 14 mL of  $\text{MgCl}_2$  ( $2.0 \text{ mol L}^{-1}$ ) was mixed with 14 mL of  $\text{H}_3\text{BO}_3$  ( $3.0 \text{ mol L}^{-1}$ ) firstly, the mixture was then supplied with DI water, and subsequently dropwise added 14 mL of  $\text{NaOH}$  ( $4.0 \text{ mol L}^{-1}$ ) under vigorous magnetic stirring, leading to 43 mL of hydrothermal precursor slurry. The precursor slurry was then transferred into a Teflon-lined stainless steel autoclave (capacity: 70 mL) at  $200^\circ\text{C}$  for 12.0 h. After the hydrothermal treatment, the autoclave was cooled down to room temperature naturally. The resultant white precipitate was washed with distilled water, filtered and dried at  $105^\circ\text{C}$  for 12.0 h, and finally collected for further characterization.

### 2.2. Reinforcement application evaluation

BOPP-D1 type resins (PetroChina Daqing Petrochemical Company, China) were selected as the matrix polymers to evaluate the reinforcement performance of the  $\text{Mg}_2\text{B}_2\text{O}_5$  nanorods. The nanorods were mixed with the BOPP-D1 resins directly by a high speed mixer (GH-10, Beijing Int. Plastics Machinery General Factory, China), after being dropwisely fed by some amount of titanate coupling agent (NDZ-101, Nanjing Shuguang Chemical Co., Ltd., China) or silane coupling agent  $\gamma$ -Aminopropyl triethoxysilane (KH-550, Gaizhou Hengda Welfare Chemical Factory, China) for surface modification. The weight ratio of the coupling agent to fillers and also that of the fillers to resins were adjusted within the range of 0–7.3% and 3.0–20%, respectively. The surface modified fillers ( $\text{Mg}_2\text{B}_2\text{O}_5$  nanorods) were fed to a torque rheocord (RC 90, HAAKE, Germany) for pellet fabrication, and then supplied to an injection molding machine (TTI-140FX, Donghua Machinery Ltd., China) for two types of samples, which were employed to a universal materials testing machine (Instron 4467, Instron, England) for tensile strength measurement and to an impact specimen notcher (Tinius Oisen Model 899, Horsham, USA) and pendulum impact tester (API, Dynisco, USA) for impact strength measurement, respectively.

### 2.3. Characterization

The structure of the product was identified by the X-ray powder diffractometer (XRD, D8-Advance, Bruker, Germany) using a  $\text{Cu K}\alpha$  radiation ( $\lambda = 1.54178 \text{ \AA}$ ), a fixed power source (40.0 kV, 40.0 mA) and an aligned silicon detector. The morphology, microstructure, and composition of the products were examined by the field emission scanning electron microscopy (SEM, JSM 7401F, JEOL, Japan) operated at an accelerating voltage of 1.0 kV, and a high resolution transmission electron microscopy (TEM, JEM-2010, JEOL, Japan) performed at an accelerating voltage of 120.0 kV. The size distribution of the nanowhiskers and nanorods was estimated by direct measuring about 200 particles from the typical SEM images.

## 3. Results and discussion

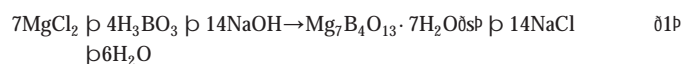
### 3.1. Kilogram-scale hydrothermal-calcination synthesis

In order to efficiently produce  $\text{MgBO}_2(\text{OH})$  nanowhiskers by the hydrothermal synthesis and  $\text{Mg}_2\text{B}_2\text{O}_5$  nanorods by the subsequent calcination in the present kilogram-scale synthesis, a relatively high solid concentration (defined as the ratio of the target product (kg) to the overall feeding volume (L)) as  $0.0548 \text{ kg/L}$  was used, as twice as that employed in the previous hydrothermal procedure for the  $\text{MgBO}_2(\text{OH})$  nanowhiskers (i.e. gram scale) [32]. Thus, the expected product in the present kilogram-scale synthesis was scaled up as ca. 4650 times as those acquired in the gram-scale hydrothermal synthesis [32], taking into consideration the variation of the overall feeding volume as well as the solid concentration between the above two

synthetic routes. Finally, 3.75 kg of  $\text{Mg}_2\text{B}_2\text{O}_5$  nanorods containing partial byproduct NaCl were obtained. It was worth noting that however, a relatively mild hydrothermal synthesis at 200 °C for 12.0 h was employed to ensure the operation security, as well as to reduce the potential corrosion of the reaction induced by the high concentration of  $\text{Cl}^-$  in the 150 L stainless steel autoclave.

### 3.2. Characterization of the $\text{MgBO}_2(\text{OH})$ nanowhiskers and $\text{Mg}_2\text{B}_2\text{O}_5$ nanorods

The structure (Fig. 2a<sub>1</sub>–a<sub>2</sub>) and morphology (Fig. 2b, c<sub>1</sub>–c<sub>3</sub>) of the kilogram-scale (Fig. 2a<sub>1</sub>, b, c<sub>1</sub>–c<sub>2</sub>) and gram-scale (Fig. 2a<sub>2</sub>, c<sub>3</sub>) hydrothermal products grown with the same operation parameters (including the concentration of the reactants, the hydrothermal temperature, and the growth time) were illustrated in Fig. 2. The as-obtained product derived from the kilogram-scale hydrothermal synthesis was dominantly consisted of monoclinic  $\text{MgBO}_2(\text{OH})$  phase (PDF No.39-1370), in accordance with that obtained by the gram-scale synthesis. The room temperature coprecipitation and hydrothermal process were described as in Eq. (1) and (2), respectively, as follows:



Although the wet powder of the hydrothermal product (Fig. 2b) had been washed for several times in the centrifuge, there still existed some residual byproduct NaCl (Fig. 2a<sub>1</sub>) originating from the room temperature coprecipitation (Eq. (1)), as well as proved by the block particles denoted by the red dotted circle in Fig. 2c<sub>1</sub>. The difficulty for NaCl washing and elimination was largely due to the relatively high solid concentration, which led to the embedment and agglomeration of the  $\text{MgBO}_2(\text{OH})$  nanowhiskers with NaCl particles. The kilogram-

scale hydrothermally synthesized  $\text{MgBO}_2(\text{OH})$  nanowhiskers exhibited good crystallinity (Fig. 2a<sub>1</sub>) with a length of 0.3–1.5  $\mu\text{m}$  and an aspect ratio of 10–30 (Fig. 2c<sub>1</sub>–c<sub>2</sub>). Meanwhile, the general head to head attached growth phenomena of the  $\text{MgBO}_2(\text{OH})$  nanowhiskers (Fig. 2c<sub>2</sub>) were quite similar to those existed for the  $\text{MgBO}_2(\text{OH})$  nanowhiskers grown by the successive effect of rolling up, oriented attachment, and Ostwald ripening mechanisms [33]. Comparatively, the gram-scale hydrothermal synthesis performed at the same hydrothermal conditions resulted in a pure phase of monoclinic  $\text{MgBO}_2(\text{OH})$  nanowhiskers (Fig. 2a<sub>2</sub>) with a higher crystallinity, a longer length, a higher aspect ratio and a smoother surface (Fig. 2c<sub>3</sub>). In other words, the mass produced nanowhiskers were with relatively low aspect ratio (Fig. 2c<sub>1</sub>). This was probably due to the scale-up effect, which might lead to the worsening of the mass and heat transfer of the reaction system to some extent and further influenced the 1D growth of the nanowhiskers. However, this issue could be improved and the kilogram-scale hydrothermally synthesized  $\text{MgBO}_2(\text{OH})$  nanowhiskers with longer length and higher aspect ratio could be expected by future optimization of the parameters for the hydrothermal mass production.

Calcination of the kilogram-scale hydrothermally synthesized  $\text{MgBO}_2(\text{OH})$  nanowhiskers containing residual byproduct NaCl at 700 °C for 6.0 h brought high crystallinity monoclinic  $\text{Mg}_2\text{B}_2\text{O}_5$  phase (PDF No. 86-0531) (Fig. 3a) as follows:



Macroscopically, the dry of soft paste containing kilogram-scale hydrothermally synthesized  $\text{MgBO}_2(\text{OH})$  nanowhiskers (Fig. 2b) leading to hard blocks containing nanowhiskers owing to the elimination of the adsorbed water. The subsequent thermal conversion of  $\text{MgBO}_2(\text{OH})$  nanowhiskers resulted in snowwhite fluffy blocks (Fig. 3b) containing  $\text{Mg}_2\text{B}_2\text{O}_5$  nanorods (Fig. 3c). The statistic data showed that the kilogram-scale calcined  $\text{Mg}_2\text{B}_2\text{O}_5$  nanorods had a length of 0.47–1.3  $\mu\text{m}$ , a diameter of 55–160 nm, and an aspect ratio of 3–15. The morphology of the as-calcined  $\text{Mg}_2\text{B}_2\text{O}_5$  nanorods was quite

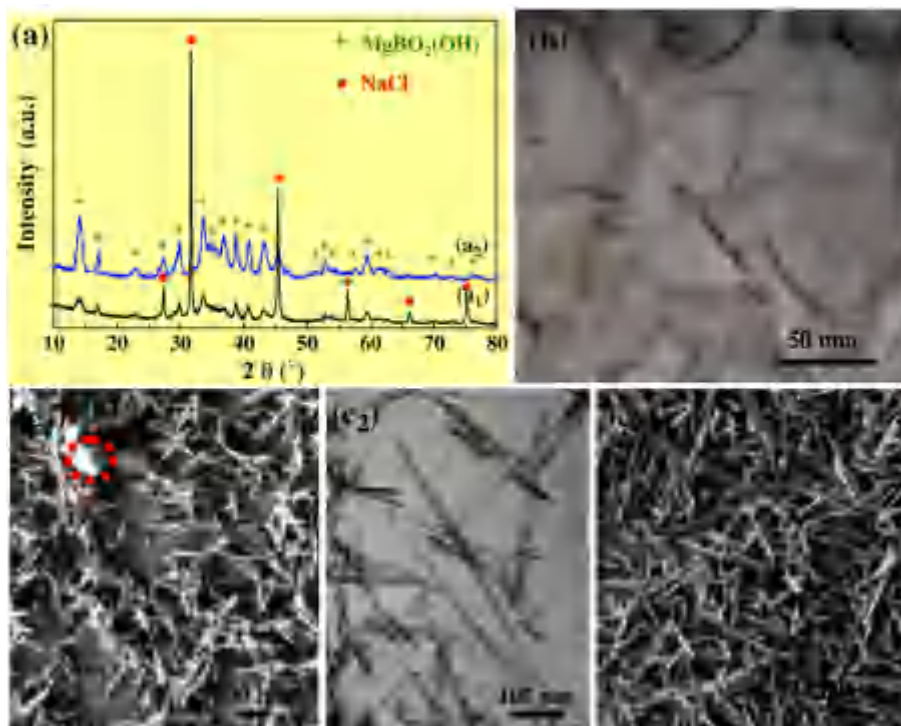


Fig. 2. Composition and morphology of the products derived from the kilogram-scale (a<sub>1</sub>, b, c<sub>1</sub>–c<sub>2</sub>) and gram-scale (a<sub>2</sub>, c<sub>3</sub>) hydrothermal synthesis performed at 200 °C for 12.0 h. (a) XRD pattern; (b) digital microscopy (wet powder); (c<sub>1</sub>, c<sub>3</sub>) SEM image; (c<sub>2</sub>) TEM image.

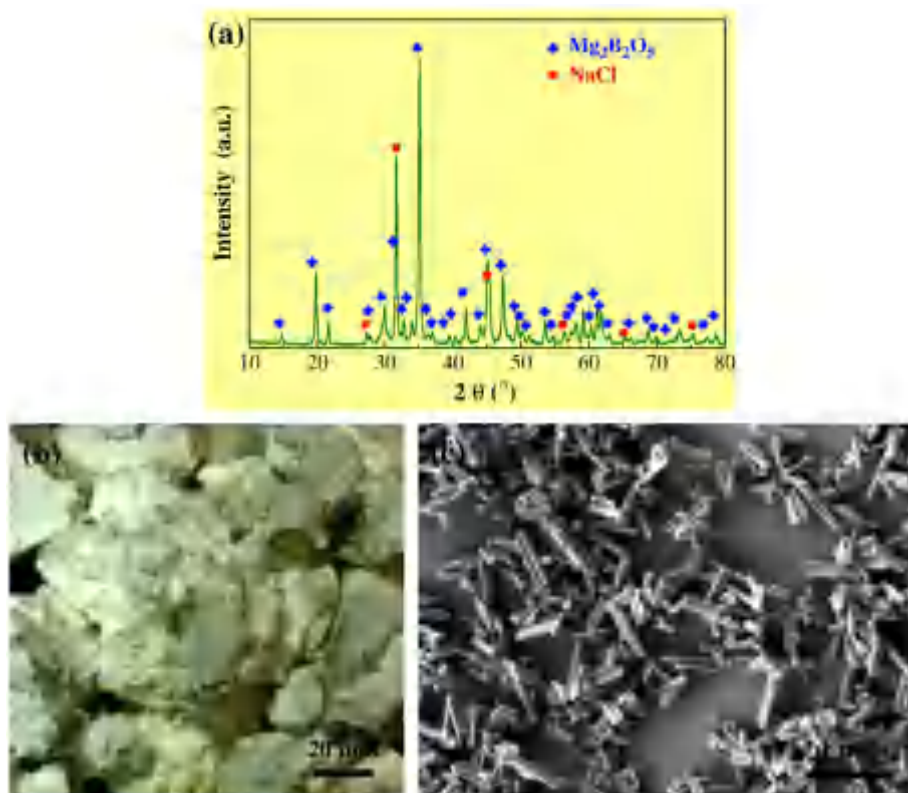


Fig. 3. Composition (a) and morphology (b–c) of the calcined product derived from the kilogram-scale hydrothermal synthesis: (a) XRD pattern; (b) Digital microscopy; (c) SEM image.

analogous to that acquired from the flux-assisted thermal conversion route [31].

Fig. 4 illustrates the microstructure of the kilogram-scale synthesized  $\text{Mg}_2\text{B}_2\text{O}_5$  nanorods. It can be seen that, the  $\text{Mg}_2\text{B}_2\text{O}_5$  nanorods had a uniform 1D morphology (Fig. 4a), without defects such as pores and cavities (Fig. 4a–b). This is quite different from the  $\text{Mg}_2\text{B}_2\text{O}_5$  nanowhiskers derived from the thermal conversion of  $\text{MgBO}_2(\text{OH})$  nanowhiskers without the aid of flux agent [34]. The selected area electron diffraction (SAED) pattern (Fig. 4c) and the high resolution TEM image (Fig. 4d) corresponding to the various sections of the same individual  $\text{Mg}_2\text{B}_2\text{O}_5$  nanorod indicated that the kilogram-scale synthesized  $\text{Mg}_2\text{B}_2\text{O}_5$  nanorods were of high crystallinity, in accordance with the XRD results (Fig. 3a). Meanwhile, three interplanar spacings (0.227, 0.437, and 0.411 nm) were detected from the explicit lattice fringes (Fig. 4d), which were quite similar to the standard values for (113), (200) (202) planes of monoclinic  $\text{Mg}_2\text{B}_2\text{O}_5$  (0.228, 0.446, and 0.408 nm), respectively. Moreover, the axial direction of the nanorod was parallel to both of the (200) and (202) planes, indicating the preferential growth of the  $\text{Mg}_2\text{B}_2\text{O}_5$  nanorods along the b axis, in well agreement with the previous results [31] and also the growth habit of the natural suanite ( $\text{Mg}_2\text{B}_2\text{O}_5$ ) [35].

### 3.3. Reinforcement performance of $\text{Mg}_2\text{B}_2\text{O}_5$ nanorods in BOPP-D1 resins

BOPP-D1 resins were widely used as the novel transparent wrappers for food, candies, cigarette, tea, syrup, milk, and dry goods, etc., due to the distinct advantages such as light weight, innocuity, dampproof, high mechanical intensity, size stability, and good printing property [36]. To explore advanced BOPP-D1 resin application in special products with a requirement, the mechanical property of BOPP-D1 resins should be improved. In order to realize the improvement of the intensity and toughness of the BOPP-D1 resins by filling the  $\text{Mg}_2\text{B}_2\text{O}_5$  nanorods, both the effect of the coupling agent on the surface of the nanorods and the compatibility between the surface

modified nanorods and the matrix materials were investigated. Table 1 shows the effect of coupling agents on the reinforcement of performance of kilogram-scale synthesized  $\text{Mg}_2\text{B}_2\text{O}_5$  nanorods in BOPP-D1 resins, with the weight ratio of the fillers (surface modified nanorods) to the matrix resins kept as 10%. Compared with the blank BOPP-D1 resins (i.e. series “zh-1”), filling the silane coupling agent KH-550 modified  $\text{Mg}_2\text{B}_2\text{O}_5$  nanorods to BOPP-D1 resins promoted the tensile strength and impact strength from 28.4 to 29.6 MPa, and 4.09 to 4.95 MPa, respectively, indicating the good compatibility between the silane coupling agent modified  $\text{Mg}_2\text{B}_2\text{O}_5$  nanorods and the matrix BOPP-D1 resins. In contrast, filling the titanate coupling agent NZD-101 modified  $\text{Mg}_2\text{B}_2\text{O}_5$  nanorods to BOPP-D1 resins led to the decrease in the tensile strength from 28.4 to 27.4 MPa on the one hand and the increase in the impact strength from 4.09 to 4.93 MPa on the other hand. Moreover, the introduction of the titanate coupling agent did not favor the improvement of the structure uniformity of the matrix BOPP-D1 resins. In addition, filling either of the two coupling agents modified  $\text{Mg}_2\text{B}_2\text{O}_5$  nanorods could improve the melt flow index of the BOPP-D1 resins, indicating the improvement of the molding flow property of the resins accordingly. Based on the above analysis, silane coupling agent was preferred to titanate coupling agent for modifying the  $\text{Mg}_2\text{B}_2\text{O}_5$  nanorods to reinforce and toughen BOPP-D1 resins in the improvement of the tensile strength, impact strength, structure uniformity, and also molding flow property.

With the silane KH-550 as the selected coupling agent, the changes of the reinforcing performance of the coupling agent modified kilogram-scale synthesized  $\text{Mg}_2\text{B}_2\text{O}_5$  nanorods in BOPP-D1 resins with the weight ratio of the coupling agent to fillers, as well as that of the fillers to resins were investigated (Table 2). It can be seen that, the silane coupling agent KH-550 modified nanorods could effectively promote both the tensile strength and impact strength. Especially, under the ratio situations of the series “zh-0” and “zh-13”, the tensile strength and impact strength of the resins were improved by 7.0–7.4% and 21.2–25.2%, respectively. When the ratio of coupling agent to

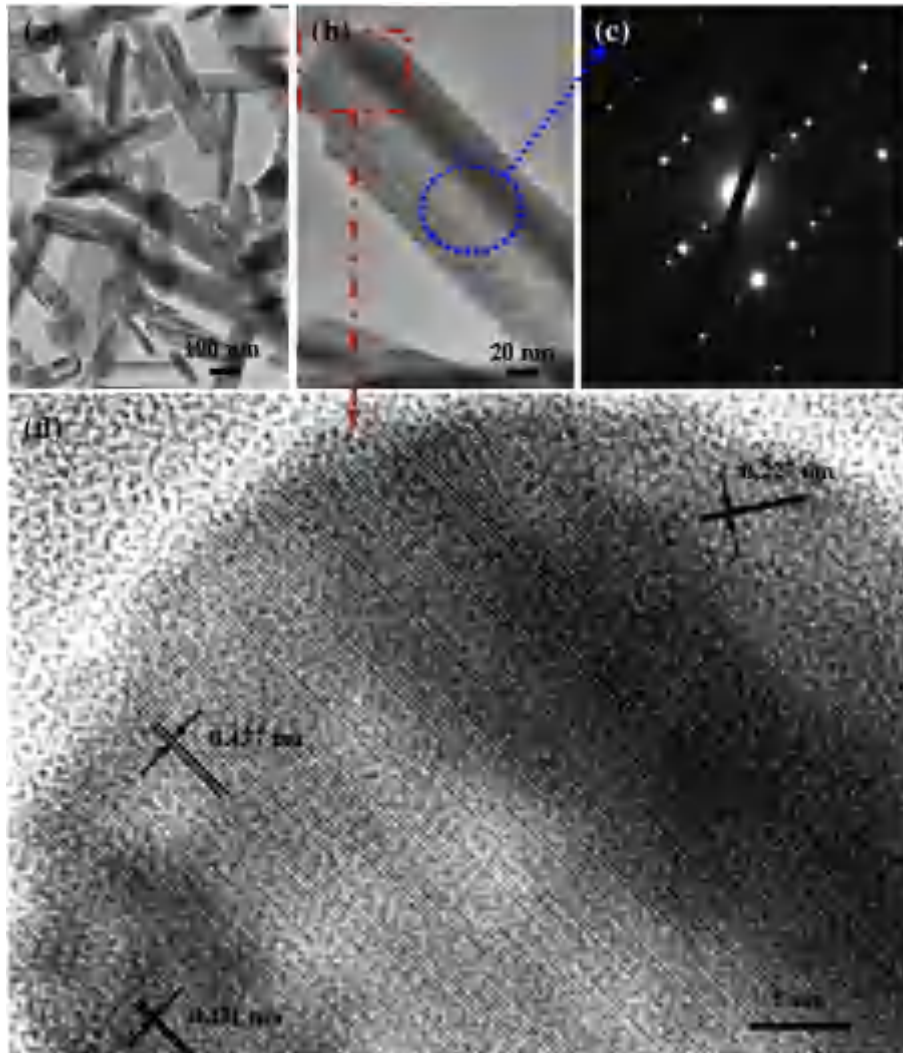


Fig. 4. TEM images (a–b), SAED pattern (c) and high resolution TEM image (d) of the calcined product derived from the kilogram-scale hydrothermal synthesis.

fillers was too low, the  $\text{Mg}_2\text{B}_2\text{O}_5$  nanorods were partially modified. In that case, the provided stress concentration points for effective stress transfer were very limited, and thus the reinforcement was not obvious. When the ratio of coupling agent to fillers was too high, the filled particles would be readily attached to each other, resulting in severe agglomeration. Such agglomeration would worsen the dispersion of the fillers in the matrix resins and further degrade the mechanical properties of the composites. Thus, the ratio of coupling agent to fillers was set within the range of 0.6–1.2 wt.%. Besides, data in Table 1 and Table 2 showed that filling the  $\text{Mg}_2\text{B}_2\text{O}_5$  nanorods modified with silane coupling agent KH-550 could reinforce and also

toughen the matrix BOPP-D1 resins, and the increase in the impact strength was higher than that in the tensile strength.

According to the data in Tables 1 and 2, variations of the tensile strength and impact strength of the BOPP-D1 resins with the ratio of fillers (surface modified nanorods) to resins under typical ratio of the silane coupling agent KH-550 to fillers are shown in Fig. 5. Under the circumstances that the ratio of the coupling agent to fillers was kept as 0.6 wt.% (Fig. 5a) and 1.2 wt.% (Fig. 5b), both the tensile strength and impact strength tended to increase first and then decrease with the increase in the ratio of fillers to resins from 3.0 wt.% to 20.0 wt.%. Meanwhile, for the aforementioned two cases of the ratio of coupling

Table 1  
Effect of coupling agent on the reinforcing performance of kilogram-scale synthesized  $\text{Mg}_2\text{B}_2\text{O}_5$  nanorods in BOPP-D1 resins.

Series	Coupling agent	Coupling agent/fillers (wt.%)	Fillers/resins (wt.%)	Tensile strength (MPa)	Impact strength ( $\text{kJ/m}^2$ )	Melt flow index (g/10 min)
zh-1 <sup>a</sup>				28.4	4.09	3.0
zh-2	Silane KH-550	1.2	10	29.6	4.95	3.6
zh-3		1.8	10	28.8	4.44	3.3
zh-4		3.5	10	28.7	5.07	2.8
zh-5		0.9	10	28.2	4.80	2.9
zh-6	Titanate NZD101	1.9	10	27.9	4.29	3.3
zh-7		2.8	10	27.4	4.93	3.5
zh-8		7.3	10	27.6	4.89	3.3

<sup>a</sup> The sample is the blank BOPP-D1 resins.

Table 2  
Reinforcing performance of silane coupling agent modified kilogram-scale synthesized  $Mg_2B_2O_5$  nanorods in BOPP-D1 resins.

Series	Coupling agent/fillers (wt.%)	Fillers/resins (wt.%)	Tensile strength (MPa)	Impact strength ( $kJ/m^2$ )
zh-0	0.6	10	30.4	4.96
zh-9	1.2	3	30.1	4.53
zh-10	1.2	5	30.2	4.55
zh-11	1.2	15	30.1	4.82
zh-12	1.2	20	28.8	4.77
zh-13	0.6	3	30.5	5.12
zh-14	0.6	5	30.2	4.09
zh-15	0.6	15	29.9	4.60
zh-16	0.6	20	29.3	4.31
zh-17	5.4	10	29.3	4.96
zh-18	0	10	30.0	4.44

agent to fillers, the appropriate ratio of fillers to resins located within the range of 8–15 wt.% and the optimal ratio of fillers to resins was ca. 10 wt.%. This was much lower than the requisite ratio 25 wt.% for  $Mg_2B_2O_5$  whiskers to reinforce Nylon-6 [37].

In addition, the kilogram-scale hydrothermal synthesis confirmed from another point of view that, a low initial reactant concentration, a high hydrothermal temperature, and a long hydrothermal time would favor the preferential growth of the anisotropic crystals with a higher

aspect ratio [33,38]. Besides, the room temperature coprecipitation byproduct NaCl could serve as the flux agent necessary for the thermal conversion of  $MgBO_2(OH)$  nanowhiskers to pore-free high crystallinity  $Mg_2B_2O_5$  nanorods [31]. It was noted that however, the  $Mg_2B_2O_5$  nanorods used in the reinforcement contained some residual NaCl, which failed to be washed out thoroughly after the calcination largely owing to the high solid concentration employed in the hydrothermal mass production. The potential negative effect of NaCl on the reinforcement performance was unclear at present, which still needed further investigation. Moreover, a more obvious reinforcing and toughening performance of the BOPP-D1 resins would be worth expecting if the kilogram scale synthesized pure phase of  $Mg_2B_2O_5$  nanorods have been well crushed, thoroughly washed and finally dried before being filled into the matrix materials, on the basis of a previous separate and more systematic surface modification study. In particular, with the hydrothermal process optimized so as to solve the corrosion problem of  $Cl^-$ , the pilot test could be successfully performed under the previous optimal gram-scale hydrothermal conditions [32], then longer and higher aspect ratio  $Mg_2B_2O_5$  nanorods even nanowhiskers would be acquired. In that case, more significant improvement of the reinforcing and toughening performance of the BOPP-D1 resins filled by  $Mg_2B_2O_5$  nanorods would be realized.

#### 4. Conclusions

In conclusion,  $MgBO_2(OH)$  nanowhiskers and  $Mg_2B_2O_5$  nanorods were hydrothermally synthesized in a kilogram scale within a 150 L stainless steel autoclave followed by thermal conversion, by using  $MgCl_2 \cdot 6H_2O$ ,  $H_3BO_3$  and NaOH as the raw materials. The kilogram-scale hydrothermal synthesis was performed at 200 °C for 12.0 h, leading to  $MgBO_2(OH)$  nanowhiskers bearing a strength of 0.3–1.5  $\mu m$  and an aspect ratio of 10–30. The thermal conversion of the kilogram-scale hydrothermally synthesized  $MgBO_2(OH)$  nanowhiskers at 700 °C for 6.0 h resulted in 3.75 kg of high crystallinity monoclinic  $Mg_2B_2O_5$  nanorods, with a length of 0.47–1.3  $\mu m$ , a diameter of 55–160 nm, an aspect ratio of 3–15, and a preferential growth along the b axis. The reinforcement application evaluation showed that, filling the silane coupling agent KH-550 modified  $Mg_2B_2O_5$  nanorods into the BOPP-D1 resins led to the increase in the tensile strength, impact strength and also melt flow index of the composites. The appropriate ratio of coupling agent to fillers (surface modified nanorods) and ratio of fillers to resins were determined within the range of 0.6–1.2 wt.% and 8–15 wt.%, respectively, and the optimal ratio of fillers to resins was ca. 10 wt.%. When the ratio of coupling agent to fillers was kept as 0.6 wt.%, the tensile strength and impact strength were increased by 7% and 21%, respectively. While the ratio of coupling agent to fillers was kept as 1.2 wt.%, the tensile strength and impact strength were increased by 4% and 21%, respectively. The present mass production of  $MgBO_2(OH)$  nanowhiskers and  $Mg_2B_2O_5$  nanorods is believed to be helpful for enlarging and propelling the great potential applications of the 1D magnesium borate nanostructures in the near future. Moreover, it provided further deep understanding for hydrothermal mass production of other 1D nanomaterials. To significantly push the scale up of hydrothermal process, some aspects should be paid enough attention in future research, such as operating safety, corrosion of the reactant system, scale-up effect, and also product purification, etc.

#### Acknowledgements

This work was supported by the Natural Science Foundation of China (NSFC, No. 50874066) and State Key Laboratory of Chemical Engineering (No. SKL-ChE-09A02). The authors thank Academe of PetroChina Daqing Petrochemical Company, China, for the support of application evaluation of  $Mg_2B_2O_5$  nanorods, and also appreciate the

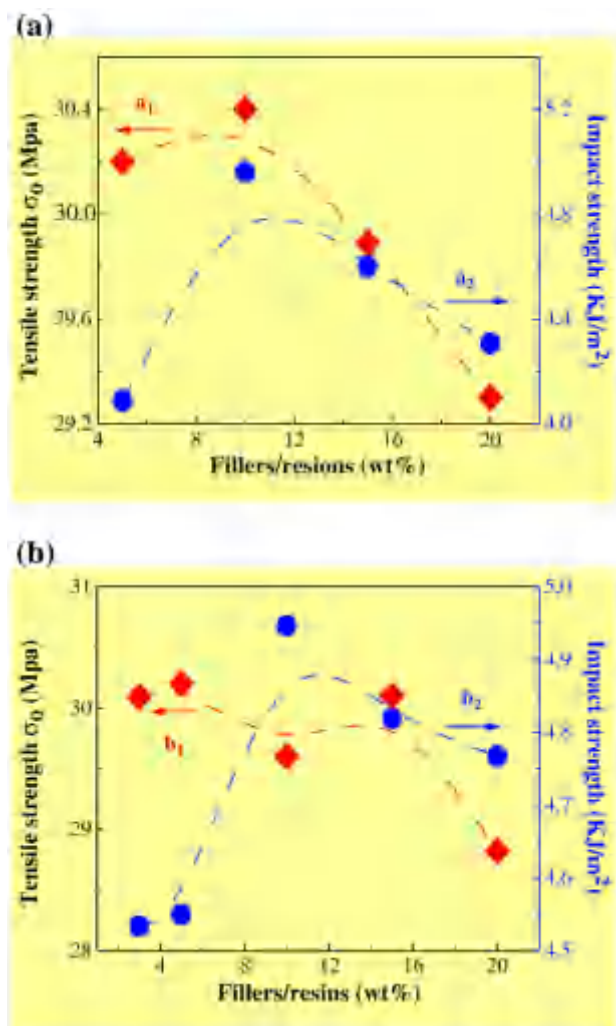


Fig. 5. Variation of the tensile strength and impact strength of the  $Mg_2B_2O_5$  nanorods reinforced BOPP-D1 resins with the ratio of fillers to resins. Percentage of the silane coupling agent in fillers: (a) 0.6 wt.%; (b) 1.2 wt.%.

reviewers for the constructive suggestions on the great improvement of the work.

## References

- [1] J.Q. Jiao, X. Liu, W. Gao, C.W. Wang, H.J. Feng, X.L. Zhao, L.P. Chen, *CrystEngComm* 11 (2009) 1886–1891.
- [2] M.T. Byrne, Y.K. Gun'ko, *Adv Mater* 22 (2010) 1672–1688.
- [3] D.S. Su, *ChemSusChem* 3 (2010) 169–180.
- [4] C. Liu, F. Li, L.P. Ma, H.M. Cheng, *Adv Mater* 22 (2010) E28–E62.
- [5] D.S. Su, R. Schlogl, *ChemSusChem* 3 (2010) 136–168.
- [6] R.Z. Ma, Y. Bando, T. Sato, *Appl Phys Lett* 81 (2002) 3467–3469.
- [7] R.Z. Ma, Y. Bando, D. Golberg, T. Sato, *Angew Chem Int Ed* 42 (2003) 1836–1838.
- [8] J. Zhang, Y.M. Zhao, *Acta Phys-Chim Sin* 22 (2006) 110–113.
- [9] Y. Li, Z.Y. Fan, J.G. Lu, R.P.H. Chang, *Chem Mater* 16 (2004) 2512–2514.
- [10] Y. Zeng, H.B. Yang, W.Y. Fu, L. Qiao, L.X. Chang, J.J. Chen, H.Y. Zhu, M.H. Li, G.T. Zou, *Mater Res Bull* 43 (2008) 2239–2247.
- [11] E.M. Elssfah, A. Elsanousi, J. Zhang, H.S. Song, C.C. Tang, *Mater Lett* 61 (2007) 4358–4361.
- [12] K. Sakane, T. Kitamura, H. Wada, M. Suzue, *Adv Powder Technol* 3 (1992) 39–46.
- [13] P.L. Wu, Z. Tian, L.D. Wang, W.D. Fei, *Thermochim Acta* 455 (2007) 7–10.
- [14] S.H. Chen, P.P. Jin, G. Schumacher, N. Wanderka, *Compos Sci Technol* 70 (2010) 123–129.
- [15] F. Wei, Q. Zhang, W.Z. Qian, H. Yu, Y. Wang, G.H. Luo, G.H. Xu, D.Z. Wang, *Powder Technol* 183 (2008) 10–20.
- [16] Q.L. Wu, L. Xiang, Y. Jin, *Powder Technol* 165 (2006) 100–104.
- [17] J.F. Chen, L. Shao, *J Chem Eng Jpn* 40 (2007) 896–904.
- [18] D.F. Xue, X.X. Yan, L. Wang, *Powder Technol* 191 (2009) 98–106.
- [19] Q. Zhang, H. Yu, Y. Liu, W.Z. Qian, Y. Wang, G.H. Luo, F. Wei, *Nano* 3 (2008) 45–50.
- [20] Y. Wang, F. Wei, G.H. Luo, H. Yu, G.S. Gu, *Chem Phys Lett* 364 (2002) 568–572.
- [21] Q. Zhang, M.Q. Zhao, J.Q. Huang, Y. Liu, Y. Wang, W.Z. Qian, F. Wei, *Carbon* 47 (2009) 2600–2610.
- [22] Q. Zhang, M.Q. Zhao, J.Q. Huang, J.Q. Nie, F. Wei, *Carbon* 48 (2010) 1196–1209.
- [23] W.C. Zhu, J.F. Chen, Y.H. Wang, *Chinese J Chem Phys* 17 (2004) 175–178.
- [24] M. Wang, H.K. Zou, L. Shao, J.F. Chen, *Powder Technol* 142 (2004) 166–174.
- [25] Y.G. Wang, M. Sakurai, M. Aono, *Nanotechnology* 19 (2008) 245610.
- [26] M.Y. Choi, H.K. Park, M.J. Jin, D.H. Yoon, S.W. Kim, *J Cryst Growth* 311 (2009) 504–507.
- [27] X. Wang, Q. Peng, Y.D. Li, *Acc Chem Res* 40 (2007) 635–643.
- [28] M. Yoshimura, K. Byrappa, *J Mater Sci* 43 (2008) 2085–2103.
- [29] C.L. Yan, L.J. Zou, J.S. Xu, J.S. Wu, F. Liu, C. Luo, D.F. Xue, *Powder Technol* 183 (2008) 2–9.
- [30] C.X. Zhao, Y.X. Yang, W. Chen, H.T. Wang, D.Y. Zhao, P.A. Webley, *CrystEngComm* 11 (2009) 739–742.
- [31] W.C. Zhu, Q. Zhang, L. Xiang, F. Wei, X.T. Sun, X.L. Piao, S.L. Zhu, *Cryst Growth Des* 8 (2008) 2938–2945.
- [32] W.C. Zhu, L. Xiang, T.B. He, S.L. Zhu, *Chem Lett* 35 (2006) 1158–1159.
- [33] W.C. Zhu, S.L. Zhu, L. Xiang, *CrystEngComm* 11 (2009) 1910–1919.
- [34] W.C. Zhu, L. Xiang, Q. Zhang, X.Y. Zhang, L. Hu, S.L. Zhu, *J Cryst Growth* 310 (2008) 4262–4267.
- [35] X.D. Xie, M.P. Zheng, L.B. Liu, *Borates Minerals*. Beijing, Science Press, 1965 in Chinese.
- [36] Y.J. Lin, P. Dias, H.Y. Chen, A. Hiltner, E. Baer, *Polymer* 49 (2008) 2578–2586.
- [37] H. Li, S. Zhang, Y. Zhang, G. Wang, *New Chem Mater* 9 (2001) 16–18 in Chinese.
- [38] W.C. Zhu, X.Y. Zhang, L. Xiang, S.L. Zhu, *Nanoscale Res Lett* 4 (2009) 724–731.